

Manifestation of Induction and Induced Polarization in the Case of Axial and Symmetrical Electrical Arrays

E.V. Ageenkova^{a,b,✉}, A.A. Sitnikov^a, I.Yu. Pesterev^a, A.V. Popkov^a

^a OOO Sibirskaya Geofizicheskaya Nauchno-Proizvodstvennaya Kompaniya, ul. Shchapova 14, Irkutsk, 664044, Russia

^b Irkutsk National Research Technical University, ul. Lermontova 83, Irkutsk, 664074, Russia

Received 18 September 2018; received in revised form 25 July 2019; accepted 28 August 2019

Abstract—The paper considers the manifestation of electromagnetic (EM) signal over the conducting polarizable ground on the measuring lines located on the axis of the source and inside it (for the symmetric Schlumberger installation). The research is based on a numerical experiment. Calculations of the EM response from one-dimensional models were carried out. The polarizability is taken into account by the frequency-dependent resistivity, using the Cole-Cole model. We describe the results of a numerical experiment on calculation of the induction signal over a conductive polarizable medium on grounded 2- and 3-electrode measuring lines located in the axial and equatorial zones of the source. It is shown that the induced polarization and the polarization associated with galvanic and eddy current are manifested in different ways.

Keywords: electromagnetic sounding, grounded electrical line, grounded 3-electrode measuring line, sounding of conductive polarizable media, Cole-Cole model, inductive induced polarization (IIP), galvanic induced polarization (GIP), forward modeling for a conductive polarizable medium.

INTRODUCTION

A geological medium from the standpoint of modern geoelectrics is a multiphase heterogeneous formation with dispersion of EM properties. A number of relaxation processes are accompanied by an EM signal superimposed on an inductive EM transient signal. A common signal can be detected by electrical exploration meters on the surface of the medium or inside of it.

Investigating the EM signal associated with relaxation processes using various electrical exploration methods allows one to obtain additional information on the properties of the geological medium: porosity, humidity, the degree of particle sorting or the presence of frozen formations or impurities, and the effects of hydrocarbons.

An artificial pulsed source of an EM field is used in electrical exploration to excite a transient in a geological medium, accompanied by relaxation processes. The most common artificial sources are a grounded electric line and an inductive (ungrounded) loop, with their impact on the medium under study being different. The grounded line in a pulsed mode creates a galvanic and eddy current in a conducting medium. The loop acts only inductively, creating an eddy current. These currents cause changes in the medium, which, when the medium returns to its initial equilibrium

state, are accompanied by EM signals characterizing these processes. Accordingly, for a grounded line, there are induced polarization (IP) processes associated with both galvanic and eddy currents. For the loop, there are relaxation processes associated only with eddy current. The meters display the common signal.

The manifestation of an IP signal after a pulsed impact for electric lines located in the axial (Komarov, 1980) and equatorial (Vishnyakov et al., 1988; Petrov, 2000) regions of the source has been studied repeatedly, but no one has distinguished which current gives rise to relaxation processes – galvanic, eddy, or both.

The manifestation of an inductive induced polarization (IIP) signal was studied for an inductive array (Kompaniets et al., 2013; Kozhevnikov et al., 2014; Kamenetsky et al., 2014; Hallbauer-Zadorozhnaya, 2016), and this issue for grounded electric lines was investigated to a much smaller extent (Legeydo, 1998; Moiseev, 2002). Legeydo proposed a number of geoelectrical models based on the geological conditions of the south of the Siberian platform, in which IP was associated with galvanic and eddy currents. That issue was developed by numerical simulation for axial and symmetric electrical arrays, and this work described the simulation results and suggested how to interpret them.

A more complex transient from a grounded line source requires detailed consideration. The induction and the IP associated with galvanic and eddy currents manifest themselves in different ways on meters located in the axial and

✉ Corresponding author.

E-mail address: alv@dnme.ru (E.V. Ageenkova)

equatorial regions of the source. Such differences should be known for properly planning field measurements and understanding their results.

The EM field during the transient is calculated on 2- and 3-electrode (Legeydo et al., 1995, 1997) measuring lines. A transient signal is calculated for 2 and 3-electrode lines, and the second final difference of the transient signal and the EM field transform is their ratio (Legeydo et al., 1995, 1997). It is known that such transformation of the signals measured in the axial region of the source can reduce the manifestation of the induction component of the transient at the late stage of the transient. From this point on, the behavior of the transform is determined by GIP. The description of the manifestation in the transform of a signal associated with IIP is another task that this study faces.

A MULTIPHASE HETEROGENEOUS MEDIUM

In a geological medium, an alternating EM field propagates diffusely, and the penetration of the field into the ground is accompanied by the formation of an eddy current and a secondary EM field. The eddy current flow causes a number of different processes of charge separation. Along with the decay of the eddy current, relaxation processes occur as an EM signal due to heat losses.

The flowing of galvanic current in this medium is accompanied by similar phenomena, ultimately manifesting themselves as an EM signal.

From the standpoint of modern geoelectrics, a geological medium seems to be a conducting multiphase heterogeneous formation with dispersion of EM properties, which is caused by a series of relaxation processes (inertial processes characterized by relaxation times) at phase boundaries or inside of regions with contrasting changes in EM properties.

The dispersion of EM properties, which manifests itself in electrical exploration measurements in different ranges of recording time (or frequency ranges), has several denotations in geoelectrics: the effect of induced polarization (IP) or low-frequency dispersion (LFD) (Kamenetskii, 1997), the Maxwell–Wagner relaxation (Sidorov, 1987; Gubatenko, 1991) the Debye dielectric relaxation (Kozhevnikov, 2012), and orientational polarization inherent in dielectrics (Auzin and Zatsepin, 2015). These effects manifest themselves at times from nanoseconds – orientational polarization (Auzin and Zatsepin, 2015) to hundreds of milliseconds and seconds – IP (Komarov, 1980; Hallbauer-Zadorozhnaya, 2016).

For the described numerical experiment, the IP effects were taken into account by introducing a frequency-dependent electrical resistance (ER). The frequency dispersion of ER was described by the Cole-Cole model (1) (Mogilatov, 2014):

$$\rho(\omega) = \rho_0 \left(1 - \frac{\eta(i\omega\tau)^c}{1 + (i\omega\tau)^c} \right), \quad (1)$$

where ρ_0 is the direct-current ER (Ohm·m), η is the polarizability (unit fraction), τ is the time constant (s), c is the power exponent, and ω is the circular frequency (s^{-1}).

INDUCTIVE INDUCED POLARIZATION UPON EXCITING A TRANSIENT BY AN INDUCTIVE SOURCE

The first studies of the manifestation of an IP signal in electrometric measurements were associated with grounded electric lines, and it was mainly after the action of galvanic current on a multiphase geological medium that the manifestations of electrochemical and electrokinetic processes were recorded (Komarov, 1980; Zhdanov, 2012). In measurements by inductive arrays and pulsed excitation of the transient, nonmonotonic drops up to a change in the signal polarity were observed, which could not be described by the diffusion propagation of the EM field in a conducting medium (Kozhevnikov, 2012). The source of that effect was initially attributed to the macroscopically heterogeneous medium and associated with the manifestation of the Maxwell–Wagner effect in frozen rocks with frequency-independent conductivity (σ) and dielectric constant (ϵ) (Sidorov, 1987). Then it was shown that, in a number of cases and primarily in relation to the permafrost zone conditions, the anomalous transient characteristics could be explained within the framework of the model of a homogeneous geological medium containing substances with polar molecules and the theory of the Debye dielectric relaxation (Kozhevnikov, 2012; Kozhevnikov et al., 2014).

Inductive induced polarization occurs when an eddy current is applied to a polarized medium (Fig. 1a). Its manifestation in an EM signal is clearly visible with inductive excitation and reception of the transient (in a time range). In the results of measurements carried out via transient electromagnetic sounding (TES) with coaxial arrays, IP manifests itself as a signal of the opposite sign in contrast to the EM transient. The IIP can be associated with a number of relaxation processes of various nature. The most rapid relaxation is observed in frozen rocks. It manifests itself at times from first microseconds to first milliseconds. Electrokinetic and electrolytic processes are more inertial. The electrokinetic processes are electroosmosis and membrane polarization associated with an electric double layer (EDL) of a two-phase porous medium and changes in pore diameters. The duration of electro-space relaxation ranges from first milliseconds to hundreds of milliseconds. Membrane polarization is set from milliseconds to seconds (Hallbauer-Zadorozhnaya, 2016). Electrolytic processes are associated with the presence of electron-conductive inclusions inside a porous (fractured) geological medium. They last from first milliseconds to seconds.

The manifestation of electrophysical relaxation in inductive measurements is called fast-decaying inductive induced polarization (FIIP) (Kozhevnikov, 2012). There is evidence

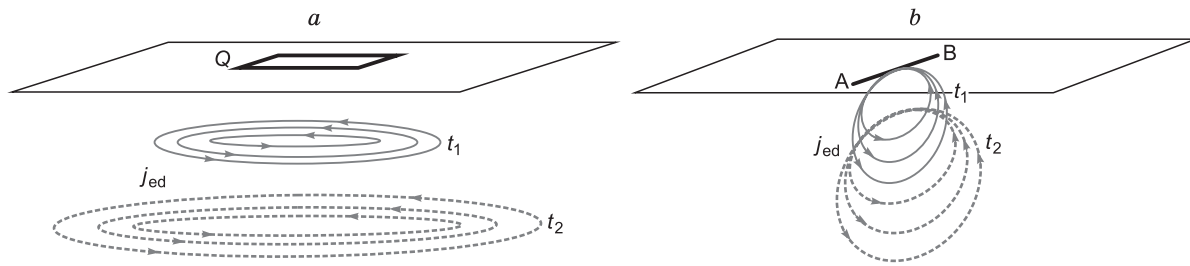


Fig. 1. Simplified structure of eddy currents: *a*, for the inductive loop source (Q); *b*, for the grounded line source (AB). j_{ed} , main eddy current density; t_1 and t_2 , instances for which the eddy current density is shown.

of fast-decaying induced polarization (FIP) in measurements with grounded lines (Karasev et al., 2005). The manifestation of electrokinetic and electrolytic relaxation is called LFD or IP (Kamenetskii, 1997).

The induction excitation and reception of an unsteady EM field is characterized by the excitation of eddy currents only, which, as they flow in a polarized medium, excite the IIP associated with relaxation processes of various nature. But the density of eddy currents is less than that of galvanic currents, and the time of their flow in the ground is less than that of galvanic currents, so such excitation and reception system is rarely used to study IP. It can be argued that the IIP processes, as a rule, are interfering with investigating induction using inductive arrays.

When it comes to inductive excitation and the reception of the EM signal of the transient, the polarization induced by an eddy current manifests itself as a change of the EMF sign.

TRANSIENT IN A CONDUCTING POLARIZED MEDIUM UNDER THE ACTION OF A PULSED SOURCE THAT IS A GROUNDED ELECTRICAL LINE

A grounded electrical line acts on a conducting polarizing medium in a slightly different way than an inductive source (Mogilatov, 2014). When a potential difference is applied to the supply electrodes, a potential EM field is established in the medium, which forms a galvanic current flow. The current density distribution in the medium depends on its conductivity along with the size of the source and decreases as the depth and horizontal distance from the source increase. The formation of galvanic current separates charges in the geological medium, which lasts for a calculable time. An IP field counteracting the potential field of the grounded source is formed. This is manifested in the changing potential difference on the meter during a current pulse after introducing the current in both the axial and equatorial regions of the source. The potential difference grows and, with a sufficient pulse duration, it can reach asymptotes – the direct-current potential differences.

During a current pulse, the current flows from electrode A to electrode B in the lower half-space (for pulses of the

same polarity) and from electrode B to electrode A in the source cable, closing the current ring. The force lines of constant magnetic field, which form the magnetic flux Φ_1 , cover the current lines. Current I flowing in the cable spreads in the lower half-space with uneven density. In the equatorial region of the source, it begins to decrease sharply at a depth of approximately $AB/2$ (Matveev, 1990). In the axial region of the source, the current density drops as the separation increases, but the depth to which the current density virtually does not decrease becomes larger along with the separation. The so-called effective depth of direct-current sounding in the axial region of the source is estimated to range from $1/4$ to $1/10$ of the separation length (Matveev, 1990).

Turning off the supply current in the medium causes changes in the currents and EM fields. The direction of the IP field becomes different, and now it has the same direction as the primary potential field of the source. The charges separated by an external current return to their original position, the GIP current begins to flow, accompanied by the formation of an EM signal. This is an inertial process or rather a series of processes of various nature, each characterized by a relaxation time, so the potential difference on the meters after turning off the current does not vanish immediately, but the IP drops (Komarov, 1980).

As the primary current is turned off, the inductive process of diffusion of the eddy current occurs in the conducting medium. Turning off the galvanic current flowing in the cable and in the ground is followed by a decrease in the magnetic flux Φ_1 , which penetrates this circuit. Due to the phenomenon of self-induction, the magnetic flux Φ_2 is formed, which prevents a decrease in flux Φ_1 , it is directed in the same direction as the primary flux. Flux Φ_2 induces an eddy current, its spatial distribution is identical to the structure of the galvanic current everywhere except for the equatorial region of the source, and, under the cable connecting electrodes A and B, a region is formed with the opposite direction of the high-density current, creating a current equivalent to the current in the cable at the instance of the pulse, and closing the eddy current ring. On a symmetric meter, the potential difference changes its sign to the opposite with respect to the potential difference during transmission. The sign of $\Delta U(t)$ on the meter in the axial region of the source does not change.

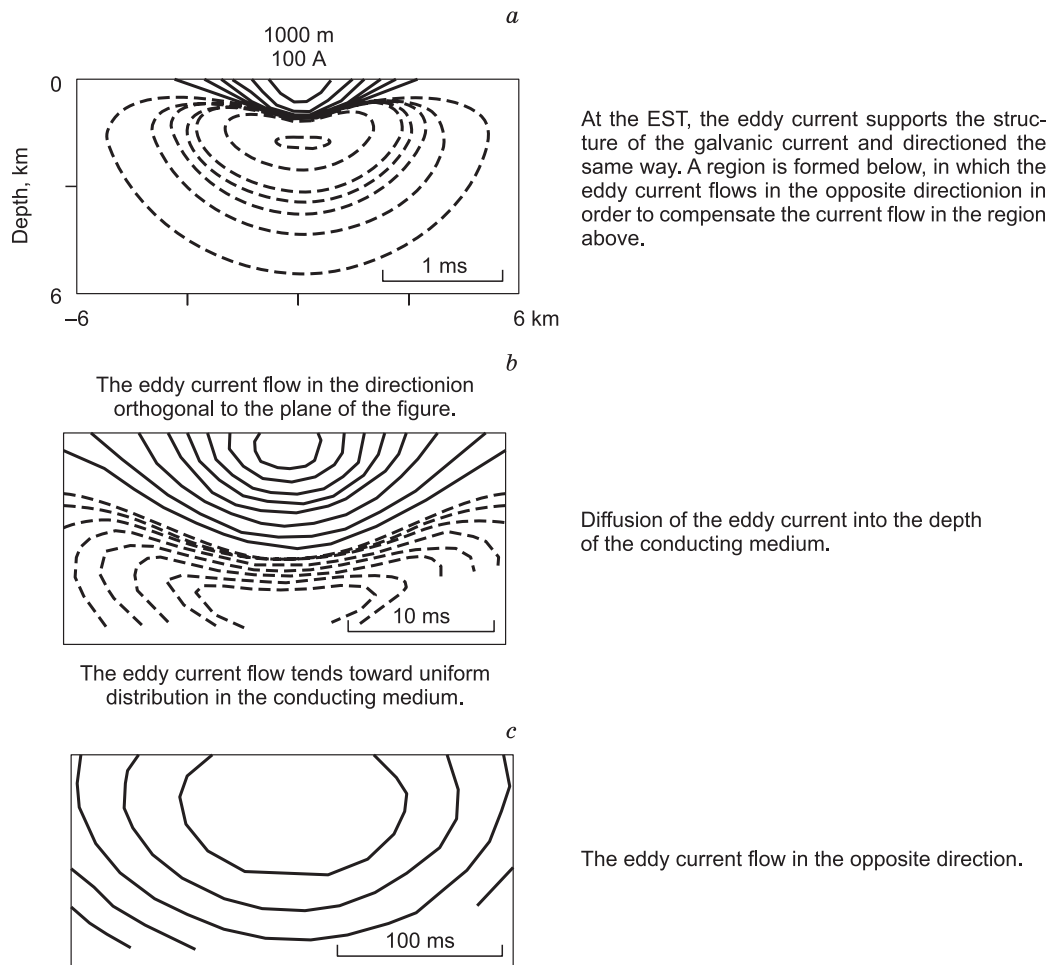


Fig. 2. Isolines of the eddy current density at different times of the transient, according to Strack (1992).

Initially, the eddy current, mainly in the region where its density is maximum, is held in a solenoidal trap by a high-frequency magnetic field, which prevents it from spreading and penetrating deeper (Matveev, 1990), and this is an early stage of the transient (EST) (Fig. 2a). As the magnetic field weakens, the current begins to seep (diffuse) into the conducting medium (in depth and in breadth), which is the EM transient (EMT) (Fig. 2b). The eddy current tends to a uniform density in the medium (Fig. 2c).

Changes in the eddy current structure for an inductive and galvanic source are visually represented by showing a ring of maximum density of the eddy current for two instances of the transient (Fig. 1). The ring of eddy currents for the source of the grounded line spreads deep into the surface mainly in a plane perpendicular to the ground surface (Strack, 1992). The eddy current ring created by an inductive loop diffuses deep into the conducting medium in a plane parallel to the ground surface (Nabighian, 1979).

The arising eddy current also separates charges in a heterogeneous multiphase geological medium, and, as it decays due to heat losses, the medium inertially returns to its initial

equilibrium state, accompanying this by a IIP current flow and the formation of an EM signal.

Thus, a grounded line in a pulsed mode in a conducting polarizing medium generates a GIP current when the source is turned on and an eddy current along with an IIP current after the source is turned off, with their flow being accompanied by an EM signal detected on the surface by the meters. The induction component of the signal is associated with a secondary EM field of the eddy current flowing in the conducting regions of the geological medium. The GIP signal is related to the galvanic current induced relaxation processes. The IIP signal is associated with the eddy current induced relaxation processes.

GROUNDING LINE METERS AND 3-ELECTRODE GROUNDING LINES

It is possible to use 3-electrode measuring lines ($M_1M_2M_3$, $M_2M_3M_4$, $M_3M_4M_5$, and $M_4M_5M_6$) to measure a transient signal between electrodes M_1-M_3 , M_2-M_4 , M_3-M_5 , and M_4-

M_6 and the second finite difference of this signal on three electrodes. Next, one may form a set of EM field transforms making it possible to suppress the contribution of the electrodynamic component at a late stage of the transient and improve the contribution of the GIP component. Based on the estimated signal of the transient between electrodes M_1 – M_2 , M_2 – M_3 , M_3 – M_4 , M_4 – M_5 , and M_5 – M_6 , it is possible to form potential difference ΔU between the first and last electrodes of each 3-electrode measuring line (2), e.g., for line $M_1M_2M_3$, and the second finite difference of the transient signal Δ^2U (3). Next, one calculates transform P1 as a ratio of Δ^2U to ΔU (4) (Legeydo et al., 1995, 1997; Legeydo, 1998).

$$\Delta U_{M_1M_3} = \Delta U_{M_1M_2} + U_{M_2M_3}, \quad (2)$$

$$\Delta^2 U_{M_1M_2M_3} = \Delta U_{M_1M_2} - \Delta U_{M_2M_3}, \quad (3)$$

$$P1_{M_1M_2M_3} = \frac{\Delta^2 U_{M_1M_2M_3}}{\Delta U_{M_1M_3}} = \frac{\Delta U_{M_1M_2} - \Delta U_{M_2M_3}}{\Delta U_{M_1M_2} + \Delta U_{M_2M_3}}. \quad (4)$$

In such a transformation, the EM field component tending to uniformity in space decreases, and that which is heterogeneous in space, on the contrary, gains more weight (become emphasized).

MANIFESTATION OF AN IP SIGNAL ASSOCIATED WITH GALVANIC AND EDDY CURRENTS ON LINES LOCATED IN THE AXIAL AND EQUATORIAL REGIONS OF THE SOURCE

For direct-current and pulsed excitation electrical arrays, there are arrays with meters in the axial or equatorial regions of the source. Arrays with measurements in the axial region are often called dipole arrays, although the separation is small and does not allow for neglecting the true size of the lines. Arrays with a meter in the equatorial region are often symmetric with respect to the center of the source.

The effective depth of direct-current sounding is estimated from a distance between the source and the meter (for measurements in the axial region of the source) and from the size of the current line (for measurements carried out by a symmetrical array).

The direct current created in the medium by a grounded electric line spreads unevenly in the lower half-space, the highest density is estimated to a depth comparable to the separation length for measurements in the axial region of the

source or to half the source length for measurements by a symmetrical installation.

It is known for the grounded line source that the measured signal of the electrodynamic transient and GIP have the same sign for a one-dimensional medium in the axial region of the source and different signs in the equatorial region (Vishnyakov et al., 1988; Petrov, 2000; Moiseev, 2002; Antonov and Shein, 2006).

Calculations are carried out for an electrical array with measurements in the axial and equatorial regions of the source (Fig. 3), consisting of source AB, several measuring lines M_1M_2 , M_2M_3 , M_3M_4 , M_4M_5 , and M_5M_6 , which are located in the axial region of the source, and measuring line MN located in the equatorial region of the source. Distances between the center of the current line and the measuring line are 1500, 2500, 3500, 4500, and 5500 m. A time range for studying the signal is limited to a value from 100 μ m to 2 s.

For this array, the effective direct-current sounding depth increases for measurements in the axial region and is estimated to be from 300 to 1100 m. For a 400 m long symmetrical line with a 1000-m long source, it equals approximately 500 m.

The galvanic current spreading in the ground from two groundings creates a potential EM field, which decreases as the distance from it becomes longer, particularly in the axial region of the source. The IP currents repeating the current distribution in the ground, which caused them, and the EM field formed by the IIP currents also remain inhomogeneous in the axial region of the source.

In the case of pulsed excitation, a change in the source current is followed by the formation of an eddy current in the conducting medium. For the source under consideration, the eddy current structure at the beginning of the transient is identical to the galvanic current structure (Fig. 1b). The transient is associated with the spreading of the ring of the main density of eddy currents downstream and in breadth (Fig. 2), so its density at the late stage is evenly distributed in the lower half-space, manifesting itself in a decrease in the spatial inhomogeneity of the inductive EM field, which becomes close to zero at the late stage of the transient.

The eddy current diffusing in the conducting medium becomes a source of charge separation. After its decay, the charges return to their original position and form an IIP current.

The transient and polarization, caused both galvanically and inductively, proceed conjointly and manifest themselves as a common EM signal on the meters. However, the spatial

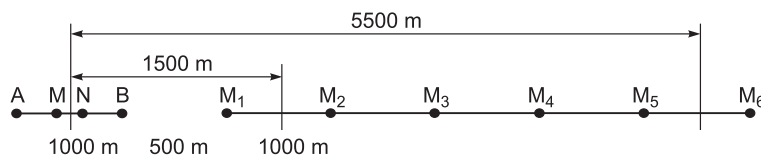


Fig. 3. Array for the numerical experiment. Measuring lines in the axial (M_1M_2 , M_2M_3 , M_3M_4 , M_4M_5 , M_5M_6) and equatorial (MN) regions of the source (AB).

Table 1. “No VP”

| Layer number | ρ , Ohm·m | η , % | h , m |
|--------------|----------------|------------|---------|
| 1 | 50 | 0 | 200 |
| 2 | 1000 | 0 | 500 |
| 3 | 20 | 0 | 200 |
| 4 | 1000 | 0 | — |

Table 2. “VPG” model

| Layer number | ρ , Ohm·m | η , % | τ , s | c | h , m |
|--------------|----------------|------------|------------|-----|---------|
| 1 | 50 | 2 | 0.5 | 0.5 | 200 |
| 2 | 1000 | 0 | — | — | 500 |
| 3 | 20 | 0 | — | — | 200 |
| 4 | 1000 | 0 | — | — | — |

density distribution of these currents and its change during the transient vary, which gives hope to distinguish components from the total measured (calculated) signal.

P.Yu. Legeydo (1998) proposed a number of geoelectric models based on the geological conditions of the south of the Siberian platform (Tables 1–4), in which the IP was associated mainly with a galvanic current (“VPG”), mainly with an eddy current (“VPI”), and with two types of current (“VPG and VPI”), as well as the model in which no IP formed (“No IP”). In a four-layer horizontally-layered geoelectric section

of the KH type, the first and third relatively conductive layers were separated by a high-resistance screen. At the base of the section, there was a nonconductive foundation. It could be assumed that the IP response from the first layer was created by a galvanic and eddy current, a conductive polarizing layer located below the screen was supposedly excited inductively, and the polarization response was inductive.

The polarization characteristics of the first and third layers differ significantly. Polarizability is 2% for the first layer and 50% for the third one. This seemingly overestimated

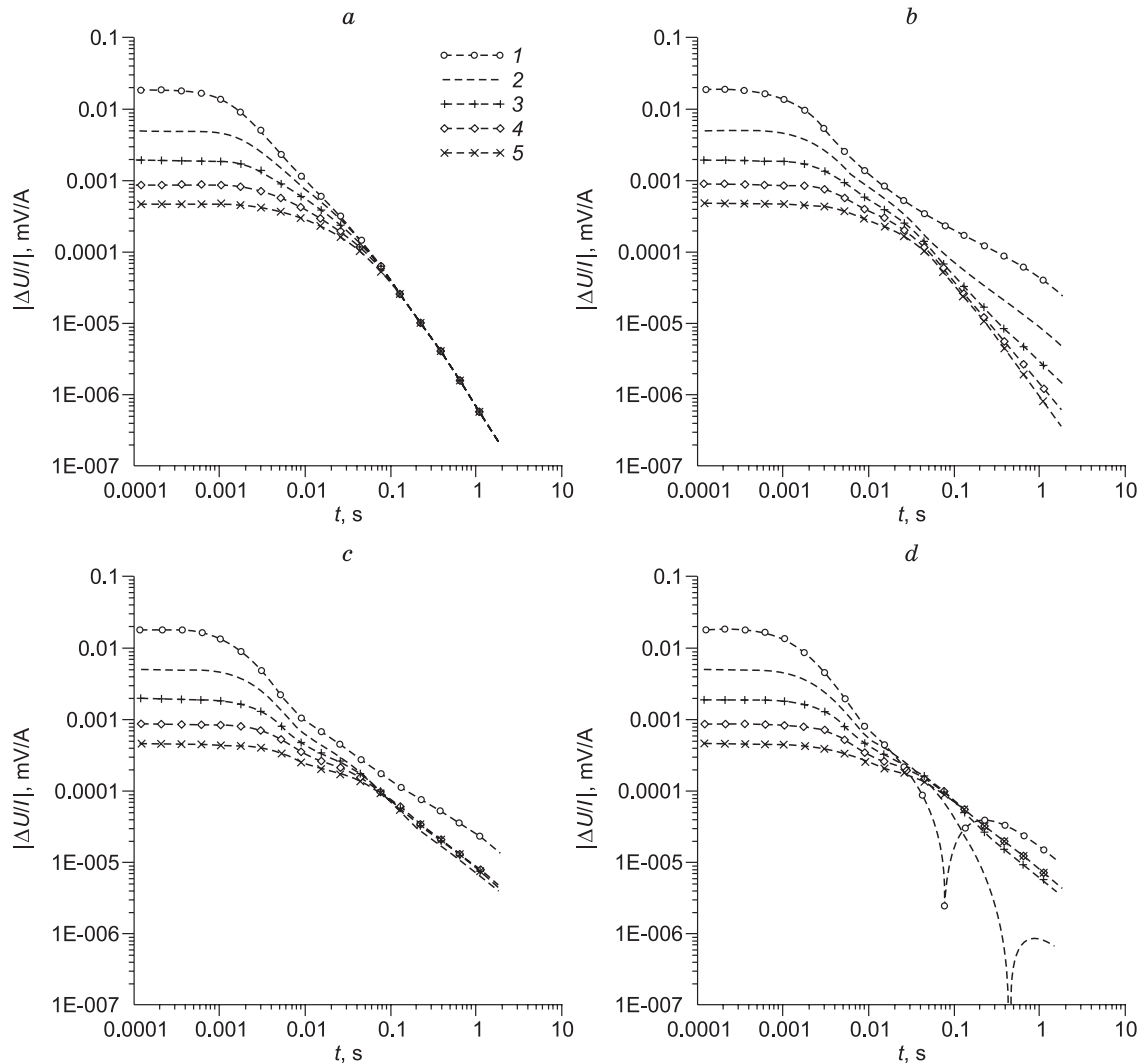


Fig. 4. Absolute values of the transient signal on the measuring lines with a separation of 1500 (1), 2500 (2), 3500 (3), 4500 (4), and 5500 (5) m: a, above the nonpolarized medium; b, above the medium polarized in the upper part of the section; c, above the polarized medium; d, above the medium polarized over the high-resistance screen.

Table 3. “VPG and VPI”

| Layer number | ρ , Ohm·m | η , % | τ , s | c | h , m |
|--------------|----------------|------------|------------|-----|---------|
| 1 | 50 | 2 | 0.5 | 0.5 | 200 |
| 2 | 1000 | 0 | — | — | 500 |
| 3 | 20 | 50 | 0.5 | 0.5 | 200 |
| 4 | 1000 | 0 | — | — | — |

polarizability of the third layer is used to increase the IP effect associated with it. Under the assumption that the polarization effect from this layer is much weaker and possibly not manifested at all against the background of the IP signal associated with the first layer, one distinguishes between the polarization components caused by the galvanic and eddy current by introducing sharply different EM properties to the under-screen thickness. This study can be considered as preliminary research into the polarization response from geological models in the waters when the polarized geological layers are overlain by a nonpolarized water column and the IP effect is associated only with them. If the water column is very thick and the source and the meter are located in the upper water layers, then the galvanic effect of the grounded source on the geological layers may be insignificant, so knowing the manifestation of IIP in a measured signal may allow correctly interpreting the measurement results.

We study the manifestations of GIP and IIP by comparing signals above a nonpolarizing medium, a medium polarized above the high-resistance second layer, a medium polarized below this layer, and a medium polarized both above and below it. These models are referred to as “No IP”, “VPG”, “VPI”, and “VPG and VPI”, respectively.

The calculations of the absolute values (modules) of the transient signal for lines M_1M_2 , M_2M_3 , M_3M_4 , M_4M_5 , and M_5M_6 , as well as the symmetric line MN are primarily shown in the graphs (Fig. 3).

For coaxial meters, a wave zone condition is fulfilled upon turning off the pulse. The meters record the response of a signal propagating through air as an EM wave and exciting an unsteady field in the ground. This signal changes only slightly: there is an asymptotic branch at early times, in a time interval from 100 μ m to 1 ms in this case. This signal behavior indicates the EST. The asymptote level depends on the separation. Above the nonpolarizing ground, the asymptote of the EST is followed by the same monotonic decrease in the transient signal on all measuring lines (Fig. 4a). After about 30 ms, the signals on all the measuring lines become almost equal, i.e., the dependence on the separation vanishes, which indicates a uniform eddy current distribution in the ground. This characterizes the late stage of the EM transient in the medium.

On line MN (Fig. 5), the transient signal has the opposite sign with respect to the primary field.

Above the ground polarized in the upper part of the section (Fig. 4b), the decline on all lines differs from that on the nonpolarized section and the difference in the transient sig-

Table 4. “VPI” model

| Layer number | ρ , Ohm·m | η , % | τ , s | c | h , m |
|--------------|----------------|------------|------------|-----|---------|
| 1 | 50 | 0 | — | — | 200 |
| 2 | 1000 | 0 | — | — | 500 |
| 3 | 20 | 50 | 0.5 | 0.5 | 200 |
| 4 | 1000 | 0 | — | — | — |

nal on them remains throughout the calculation time. On the symmetrical line MN, the signal changes its sign (from negative to positive) from a time of about 10 ms – this is how the GIP signal is manifested.

With the predominance of IIP (Fig. 4d), the transient on the meters is significantly different. The signal on the nearest measuring lines (a separation of 1500 and 2500 m) becomes smaller than that on the lines more distant from the source after a time of about 30 ms (a separation of 3500, 4500, and 5500 m), their difference increases over time, and they become negative after a time of 70 ms of ΔU in a separation of 1500 m and after a time of 300 ms of ΔU in a separation of 2500 m. On the symmetrical line, the signal sign changes similarly to the case with the previous model, except for the transient time through zero that increases and occurs at 30 ms, so it can be stated that the IP signal associated with the galvanic current is manifested this way.

An increase in the effective sounding depth by a direct-current array increases the fraction of the IP in the recorded signal, associated with a galvanic current. For meters farther from the source, the sign of the transient signal remains the same. At small distances, the polarization response of a galvanically excited medium arrives from small depths (in accordance with an estimate of the depth of direct current penetration for a dipole array), and the polarization signal associated with the eddy current arrives from large depths.

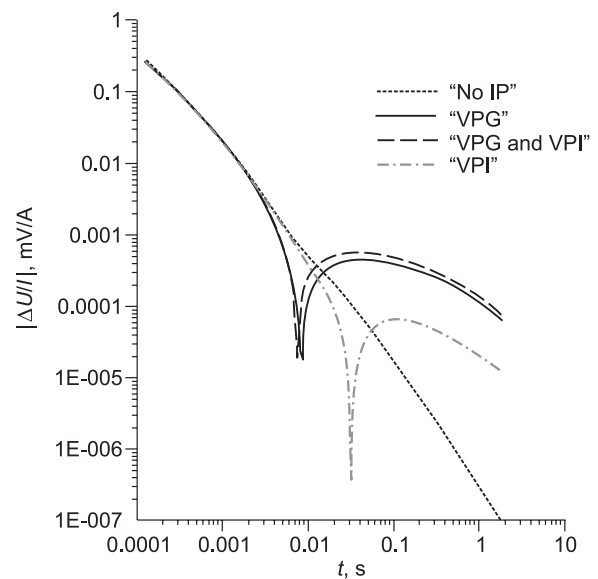


Fig. 5. Absolute values of the transient signal from four models on the symmetrical measuring line.

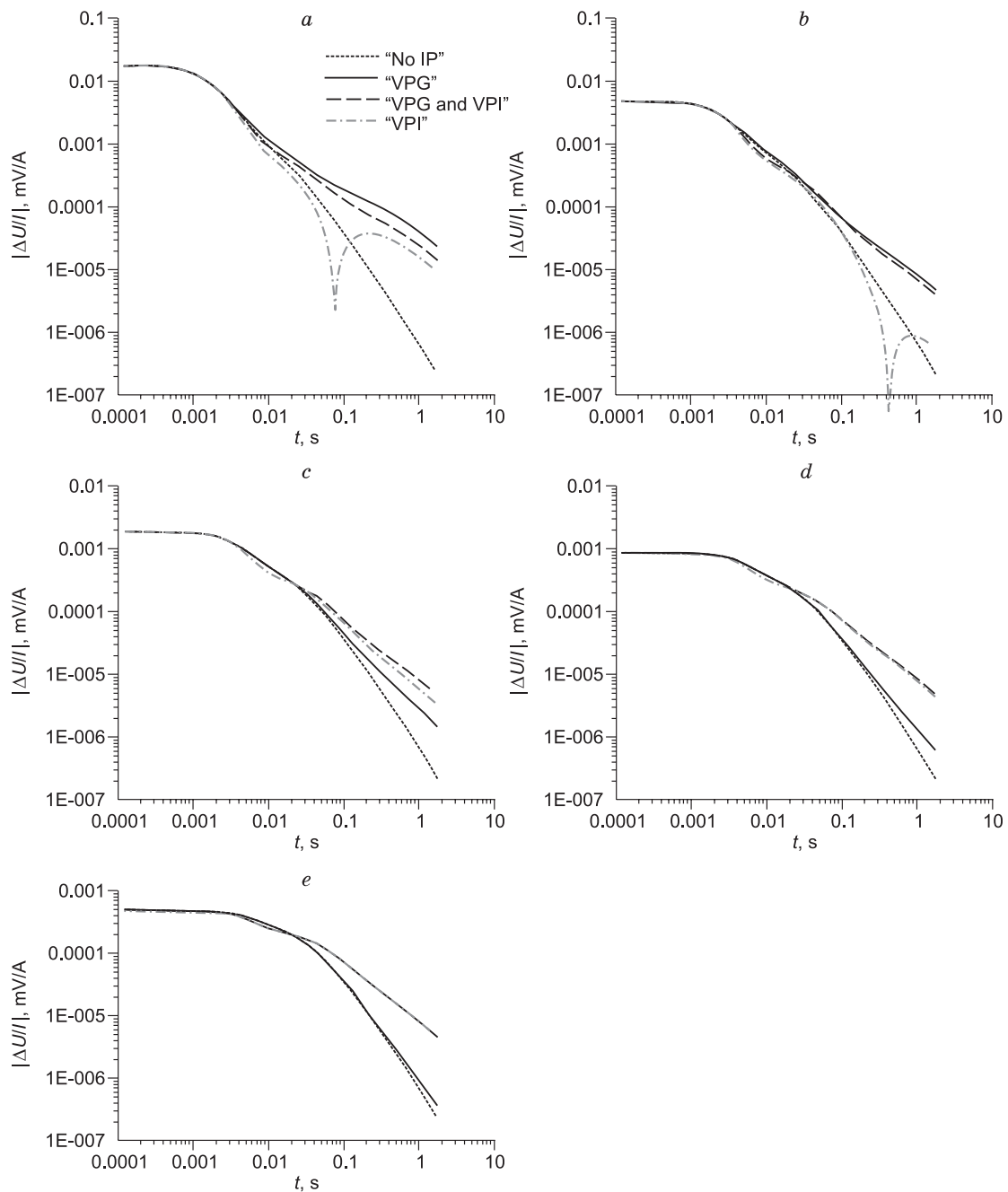


Fig. 6. Absolute values of the transient signal from four models on the measuring lines located at a distance of: a, 1500; b, 2500; c, 3500; d, 4500; e, 5500 m.

With an increase in the separation, the GIP response is recorded from large depths, and the IIP does not appear in the time range used for the calculations.

Above the model with jointly manifested GIP and IIP (Fig. 4c), the transient signal with a separation of 2500 m at a time of the order of 100 ms becomes smaller than that on the nearest and more distant measuring lines. Over time, the difference between ΔU in this separation and ΔU on other lines increases, but the sign of the potential difference before the completion of measurements (2 s) does not change on

either the second meter or the other ones. On the symmetrical line, the signal sign changes slightly earlier than that above the «VPG» model. It can be assumed that a slight increase in the time range during which the IP signal on the induction component is predominant may be caused by the combined effect of two polarized layers: the effect of superposition of the GIP and IIP signals is observed (total response).

The data can be presented differently by combining the signal modules from all models for each measuring line (Fig. 6). The graphs are given on one bilogarithmic scale.

They show differences between the signals above the non-polarized medium (dashed line), above the medium polarized in the upper part (solid lines), above the medium polarized both in the upper part and below the high-resistance screen (dashed lines), and above the medium polarized only below the high-resistance screen (dash-and-dotted lines). The differences of the signals vary depending on the separation. It is convenient to consider them against the background of a signal from a nonpolarized medium, which is the same on all separations after 50 ms. For the closest separation of 1500 m, the signal for a medium polarized under a high-resistance screen is significantly different from others. It goes through zero at a time of 70–80 ms and acquires negative values, which is why the signal above “VPG” is greater than that over “VPG and VPI”. The total signal above “VPG and VPI” decreases due to negative values of the IIP.

For a separation of 2500 m, the situation is the same, except only for the negative values of IIP becoming an order of magnitude smaller in amplitude and the transient through zero observed later (at a time of 300–400 ms). The difference in the signals of “VPG” and “VPG and VPI” is smaller too.

For a separation of 3500 m, the responses are fundamentally redistributed. The signal from the model polarized below the screen does not change sign throughout the entire calculation time. The signal from the “VPG” model after 30 ms becomes smaller than the signals from the “VPI” and “VPG and VPI” models.

For a separation of 4500 m, the signal amplitude from the “VPG” model decreases as compared to the previous separation, and the signal from the “VPI” model approaches the signal from the “VPG” and “VPG and VPI” models.

As the meter is removed from the source at 5500 m, the signal from the “VPI” model almost merges with the signal from the nonpolarized medium, and the same happens with the responses from the “VPG” and “VPG and VPI” models.

For the symmetrical array, a signal drop is observed from the earliest times. According to the interpretation of B.K. Matveev (1990), in the case of an inductive source and receiver, if the meter is located outside the ring of the maximum density of eddy currents, then it is located in the far zone (FZ) conditions, and, if it is inside of this ring, the signal recorder is in the FZ conditions. The situation is similar

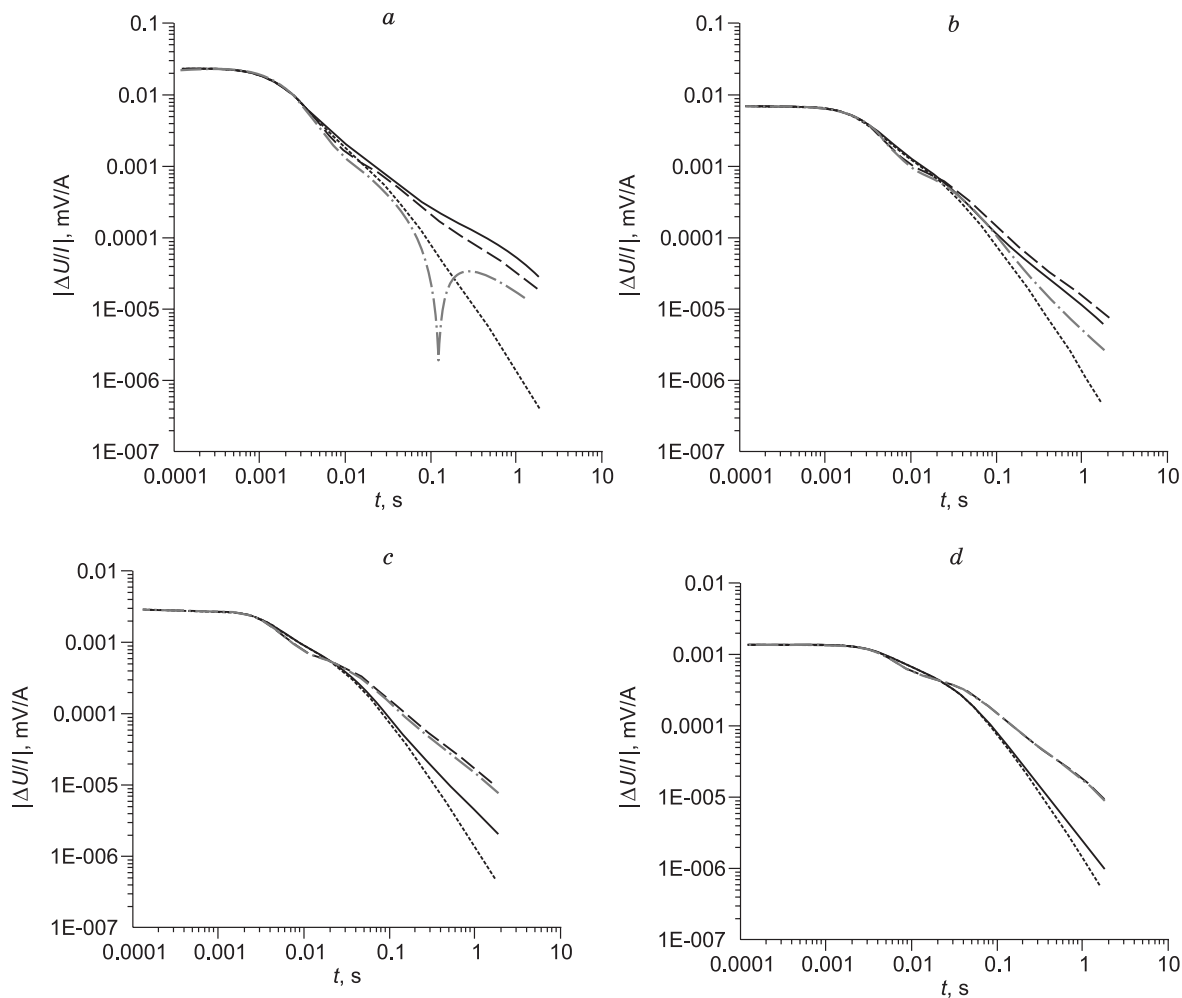


Fig. 7. Absolute values of the transient signal on the 3-electrode measuring lines $M_1M_2M_3$ (a), $M_2M_3M_4$ (b), $M_3M_4M_5$ (c), and $M_4M_5M_6$ (d). See denotations in Fig. 6.

for a grounded line, and the FZ condition is always satisfied for a symmetric meter.

During the transient, the signal sign changes on the symmetric meter for all polarized models. The IP signal has the opposite sign with respect to the exciting pulse, and, for polarized models, it changes the sign as induction decays.

The graphs (Fig. 7) for each 3-electrode measuring unit show the absolute values of the transient amplitude between the extreme electrodes of this amplitude from four models.

The response from the nonpolarized model (dashed line) at the later times is the same for all lines and the signals from other models are conveniently considered relative to this curve.

The signal change is noted only from the IIP model for a near line (M_1-M_3). With increasing separation, the “VPI” response in the later times is positive and it becomes larger in amplitude than for the first separation.

The amplitude of the “VPG” signal decreases with increasing separation at the late stage and approaches the “No IP” signal.

The “VPG and VPI” signal (dashed line) is positive for all separations and, as the separation increases and the signal

amplitude from “VPG” decreases at the late stage of the transient, the “VPI” signal tends to it.

The proximity of the potential differences on adjacent lines M_1M_2 , M_2M_3 , M_3M_4 , M_4M_5 , and M_5M_6 is indicated by the second finite difference of the transient signal ($\Delta^2 U(t)$) (Fig. 8). This value is not formed on the symmetrical array because it equals zero for a one-dimensional model. For the nonpolarized ground (dotted line), this parameter on all 3-electrode measuring lines decreases sharply after 30 ms, and its values become smaller than $1E^{-8}$ mV/A after 200 ms (not shown in Fig. 8).

For the “VPI” model (dash-and-dotted line), the sign of signal $\Delta^2 U$ for lines $M_1M_2M_3$, $M_2M_3M_4$, and $M_3M_4M_5$ changes. As the separation from the first line to the third one increases, the negative values of “VPI” in amplitude become larger than the values of “VPG”.

For the “VPG/VPI” model (dashed line), the signal sign changes on lines $M_2M_3M_4$ and $M_3M_4M_5$.

For the “VPG” model (solid line), the signal sign remains the same on all separations, but the instance at which the dip of the curves (the time at which the tilt of the curves chang-

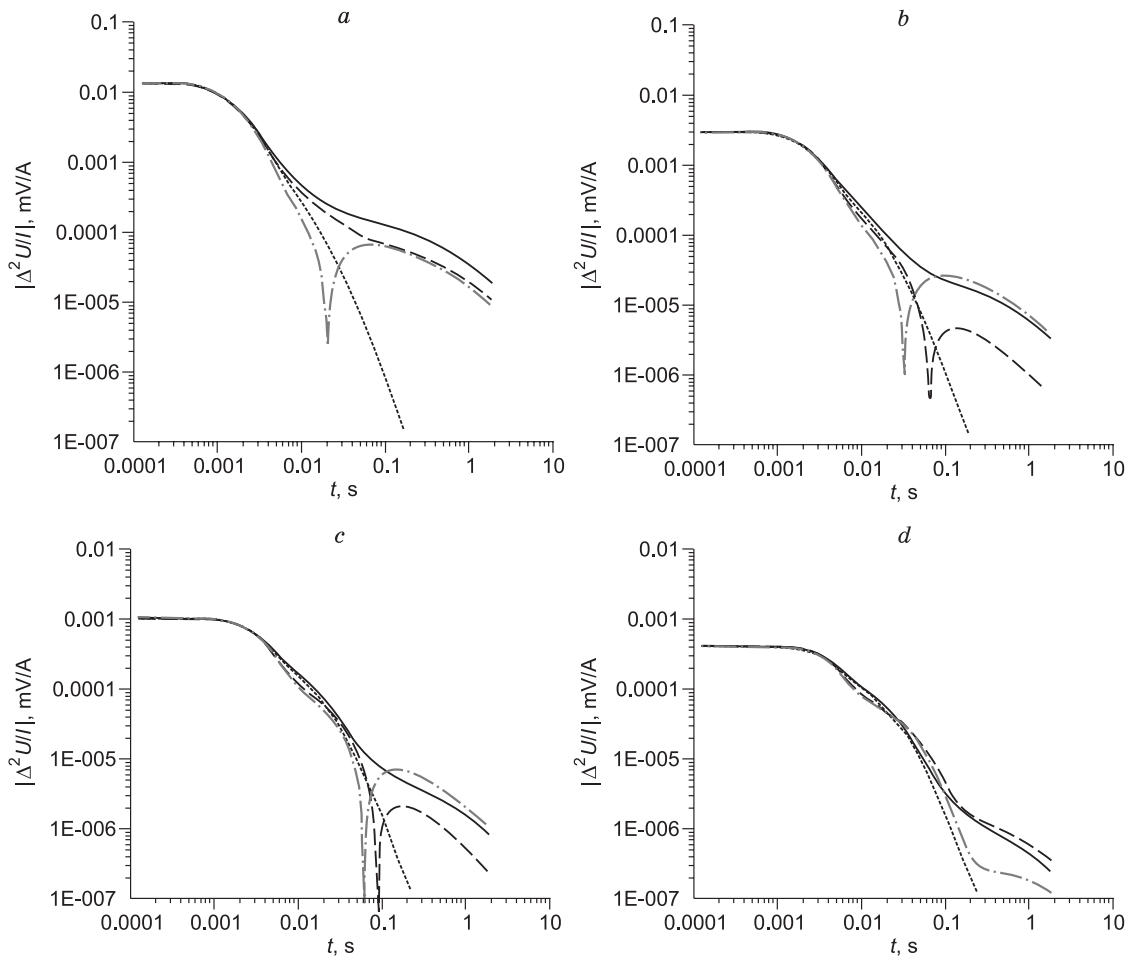


Fig. 8. Absolute values of the transient response of the second final potential difference on the 3-electrode measuring lines $M_1M_2M_3$ (a), $M_2M_3M_4$ (b), $M_3M_4M_5$ (c), and $M_4M_5M_6$ (d). See denotations in Fig. 6.

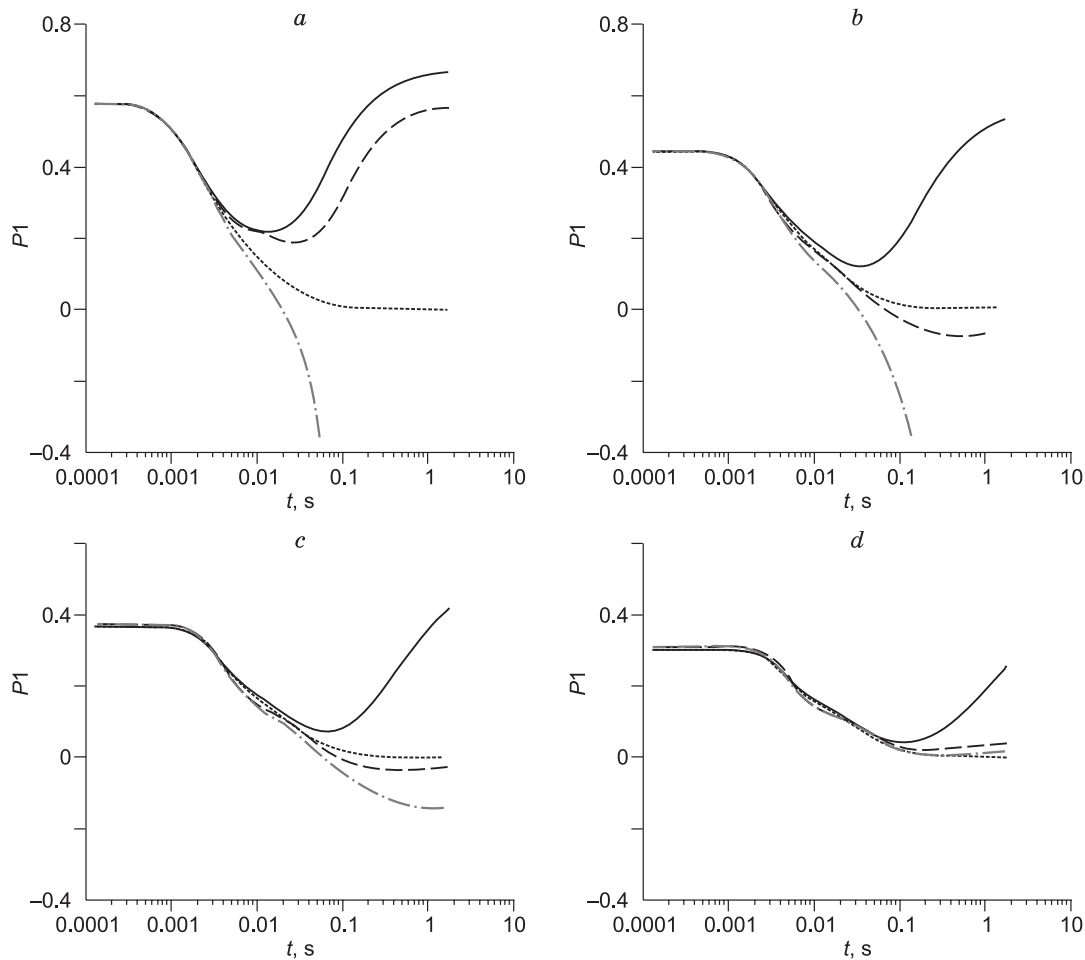


Fig. 9. Transient response of transform $P1$ on the 3- electrode measuring lines $M_1M_2M_3$ (a), $M_2M_3M_4$ (b), $M_3M_4M_5$ (c), and $M_4M_5M_6$ (d). See denotations in Fig. 6.

es with respect to the axis of time) becomes larger as the measuring line moves away from the source.

Significant changes occur in signal Δ^2U for the most distant line ($M_4M_5M_6$). On it, the signal changes at the late stage of the transient from the “VPG”, “VPG/VPI”, and “VPI” models are similar.

The graphs (Fig. 9) for each 3-electrode measuring line in the axial region of the source show transform $P1$ for the four models.

After 100 ms, the transform from the nonpolarized model (dashed line) goes to 0 at all separations, which indicates that Δ^2U tends to zero.

$P1$ for the “VPG” model (solid lines) after changing the decay rate of Δ^2U begins to increase and has an ascending right branch on all separations. The beginning of the ascending branch also shifts to later times with increasing separation.

Above the “VPI” model (dash-and-dotted line), the sign of transform $P1$, which has a descending right branch of negative values, changes after the sign of the second final potential difference becomes different on the first three lines ($M_1M_2M_3$, $M_2M_3M_4$, and $M_3M_4M_5$).

Above the model with the joint manifestation of “VPG” and “VPI” (dashed lines), a change in the sign of $P1$ is noted for the second and third lines.

INTERPRETING THE BEHAVIOR OF THE POTENTIAL DIFFERENCE ON GROUNDED LINES AND 3-ELECTRODE GROUNDED MEASURING LINES – THE MANIFESTATION OF INDUCTION, GIP, AND IIP

The calculations and various visual representations of the signal from models with different depths of location of polarized objects are carried out in order to analyze them and understand how EM signals of different origin are combined in a common transient signal in a pulsed mode of a grounded electric line.

For the near measuring line (M_1-M_3), the transient signal changes sign for the “VPI” model, and, upon removing the measurement line, the sign of signal $\Delta U(t)$ always remains positive, and, as the separation increases, the response amplitude from the “VPI” model increases. For the third line

(M_3 – M_5), the “VPI” signal exceeds the “VPG” signal and becomes close to the “VPG/VPI” signal. This behavior of the signal can be interpreted in such a way that, despite the powerful high-resistance screen, galvanic currents penetrate through it and excite the polarized under-screen thickness. As the separation increases, so does the fraction of the recorded signal, associated with the GIP from the under-screen thickness, located at a depth of 700 to 900 m. The effective depth at which the galvanic current response is recorded is approximately 400, 600, 800, and 1000 m for axial meters M_1 – M_3 , M_2 – M_4 , M_3 – M_5 , and M_4 – M_6 provided that the separation length is 1/5. It should be noted once again that the model names “VPG”, “VPI”, and “VPG/VPI” are conditional, which is clearly demonstrated by the signal described.

A change in the sign of the transient signal on lines located in the axial region of the source can be caused by the manifestation of IIP (Fig. 10).

A current pulse (CP) is followed by recording the transient signal on the measuring lines in the axial region of the source, associated with pulsed excitation propagating through air (UVZ), which decreases as the distance from the source becomes longer and dependent on the array geometry. At the EST, as the formed eddy current maintains the structure of the vanishing galvanic current, the transient signal on the meters does not decrease, which means that the eddy current density at this stage of the transient does not change for some time. After the high-frequency magnetic field that keeps the eddy current in a solenoidal loop decays (Matveev, 1990), diffusion leakage begins (spreading in depth and in breadth) in the medium of the eddy current whose density decreases, and this is reflected in a decrease in the signal on the meters in the transient time range. As soon as the eddy currents decay (their density becomes lower than the current density of GIP and IIP), the signal begins to be determined by the GIP and IIP currents. The diffusion rate of the eddy currents (transient rate) depends on the conductive properties of the geological medium, respectively, and the time at which the

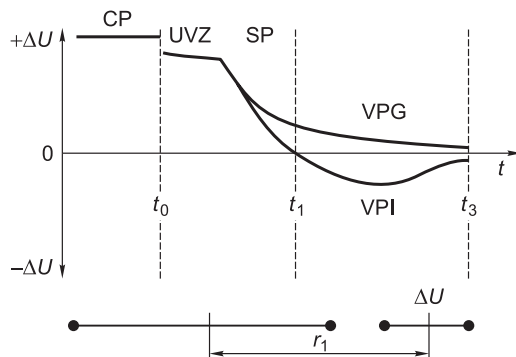


Fig. 10. Schematic of the transient over the conducting polarizing medium in the axial region of the source at small separations. CP, current pulse; UVZ, pulse excitation propagating through the air; SP, process of EM field formation; VPG, galvanic induced polarization; VPI, inductive induced polarization; t_0 , the current turn-off time; t_1 , the time at which the field sign changes with the manifestation of IIP; t_3 , end of measurements, r_1 , separation close to the size of the source.

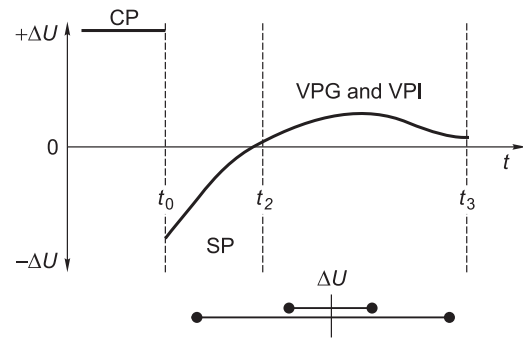


Fig. 11. Schematic of the transient over the conducting polarizing medium in the equatorial region of the source for the symmetric array. t_0 , current turn-off time; t_2 , the time at which the field sign changes with the manifestation of IP (VPG and VPI); t_3 , end of measurements. See the remaining denotations in Fig. 10.

IIP currents begin to determine the transient is also associated with this characteristic of the medium (Fig. 11).

In view of the fact that IIP is not predominant in the case of joint manifestation of GIP and IIP even if the polarizability of under-screen thickness is larger than that of over-screen thickness, the impact of GIP for the grounded line source in the case of this model is predominant over the impact of IIP, so the potential difference does not change its sign. For measurements in the axial region of the source, the sign of the induction field and the IP are the same, so the GIP is manifested as a change in the sign of the transient signal.

The manifestation of IIP and IP as a whole on this array depends on the transient time constant, the separation, and, probably, the time it takes to record the signal. If the receiver is far away from the source (Fig. 12), no IP may appear at all over a limited time range.

The appearance of transform $P1$ for the nonpolarized medium that is polarized in the upper part and under the high-resistance screen differs significantly: the transform becomes an informative tool for selecting a time range at which the signal associated with GIP or IIP is prevalent.

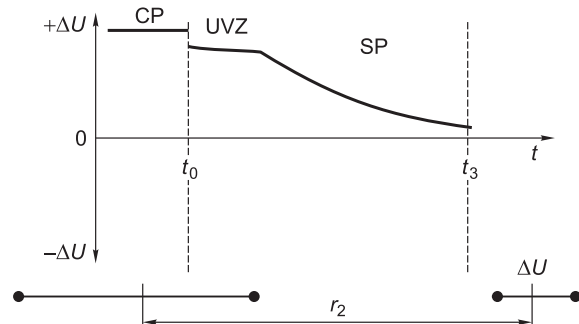


Fig. 12. Schematic of the transient over the conducting polarizing medium in the axial region of the source at large separations. See denotations in Fig. 10. r_2 , separation several times larger than the size of the source.

CONCLUSIONS

A galvanically-grounded line in pulsed current transmission in a conductive ground excites an inductive transient, GIP, and IIP. With this current pulse, various charge separation processes occur in the polarized medium. The termination of this effect is followed by inverse relaxation processes manifesting themselves as an EM signal recorded by the meter along with an EM signal associated with the diffusion of eddy currents into the conducting ground. The eddy currents propagating inside the polarized medium also induce charge separation processes, which, after weakening and decay, become reverse relaxation processes, also manifested as an additional EM signal recorded by the meter. This description of the consequences of the pulsed action of the grounded electric line on the polarized conductive ground shows that it is more complicated than with the same effect of an inductive source. The signal recorded by inductive receivers above the polarized ground contains at least an inductive and polarization component excited by an eddy current. The signal recorded by the grounded electric line contains an inductive and polarization component excited by both galvanic and eddy currents. In the signal of the polarization component, several relaxation processes of various nature may occur. Despite the complexity of the recorded signal, it is the grounded line that is most often used to study IP because the density of galvanic currents that “charge” the ground is higher than that of eddy currents of an ungrounded source, and the exposure time is determined by the duration of the current pulse and not by the duration of the transient as for an inductive source.

The interpretation of the numerical simulation results makes it possible to draw some interesting conclusions from a practical point of view. The effective depth at which the ground response is recorded by an axial installation depends on the separation, i.e., the distance between the source and the receiver. Therefore, at close distances (at small separations), the depth of direct current research is small, and, on the line grounded in the axial region of the source, the polarization caused by the eddy current manifests itself as a change in the sign of the transient signal. When the receiver is removed from the source in the axial region (increasing separation), the effective depth with which the direct current response arrives becomes larger and the impact of IIP decreases in a similar time range.

An important calculation result was the change in the sign of the transient signal for the meter in the axial region of the source in the presence of a medium for which the polarization is caused by an eddy current. This became a new scientific fact as it was believed (Moiseev, 2002) that only the second final difference of the transient signal acquired negative values. In this study, it was concluded that, in the axial region, IIP manifested itself as a change in the sign of signal $\Delta U(t)$ for the grounded line source and as a change in the sign of the second final difference of the tran-

sient signal process $\Delta^2 U(t)$ and transform $P1(t)$ for the 3-electrode measuring array.

For the symmetrical array, the transient signal has an opposite sign to the primary field, and the sign of both the GIP and IIP field matches that of the primary field.

It must be emphasized that, despite the fact that IP is excited by an eddy or galvanic current, the nature of an IIP and GIP signal is the same: electrophysical, electrochemical, and electrokinetic relaxation processes in a multiphase heterogeneous geological medium.

The focus of the research is the manifestation of IIP and GIP for water conditions. Here, the water column is a non-polarized layer whose conductivity is dependent on the water salinity, and which separates the electrical exploration unit from the conductive polarized geological medium. Depending on the water power, the depth of immersion of the array, the separation, and the time it takes to record the IIP–GIP ratio signal differ. Determining the optimal geometry for an array and the signal generation and measurement parameters to study the polarizability of a geological medium is of practical interest to aquatic (aquatorial) geoelectrics.

REFERENCES

- Antonov, E.Yu., Shein, A.N., 2007. Separation of a transient effect and induced polarization in the case of sounding of polarized media by the transient method, in: Proc. Intern. Sci. Congress “Geo-Sibir’-2007” [in Russian]. SGGGA, Novosibirsk, pp. 231–218.
- Auzin, A.A., Zatsepin, S.A., 2015. Dispersion of a dielectric constant of a geological medium (In relation to the interpretation of GIPR materials). Vestnik Voronezhskogo Gosudarstvennogo Universiteta. Seriya: Geologiya, No. 4, 122–127.
- Gubatenko, V.P., 1991. The Maxwell–Wagner effect in electrical exploration. Fizika Zemli, No. 4, 88–98.
- Hallbauer-Zadorozhnaya, V.Yu., 2016. The processes taking place in rocks when an electric current and potential difference: induced polarization. Voprosy Estestvoznaniya, No. 3 (11), 76–79.
- Kamenetskii, F.M., 1997. Electromagnetic Geophysical Studies of the Transient Method [in Russian]. GEOS, Moscow.
- Kamenetsky, F.M., Trigubovich, G.M., Chernyshev, A.V., 2014. Three Lectures on Geological Medium Induced Polarization. Vela Verlag, Munich.
- Karasev, A.P., Ptitsyn, A.B., Yuditskikh, E.Yu., 2005. Fast Transients of Induced Polarization [in Russian]. Nauka, Novosibirsk.
- Komarov, V.A., 1980. Electrical Exploration by Induced Polarization [in Russian]. Nedra, Leningrad.
- Kompaniets, S.V., Kozhevnikov, N.O., Antonov, E.Yu., 2013. The manifestation of and allowing for the inductively induced polarization in TEM sounding studies of sedimentary cover of the South of Siberian platform. Geofizika, No. 1, 35–40.
- Kozhevnikov, N.O., 2012. Fast-decaying inductive IP in frozen rocks. Russian Geology and Geophysics (Geologiya i Geofizika) 53 (4), 406–415 (527–540).
- Kozhevnikov, N.O., Antonov, E.Yu., Zakharkin, A.K., Korsakov, M.A., 2014. TEM surveys for search of taliks in areas of strong fast-decaying IP effects. Russian Geology and Geophysics (Geologiya i Geofizika) 55 (12), 1452–1460 (1815–1827).
- Legeydo, P.Yu., 1998. Theory and Technology of Differential-Normalized Geoelectrical Exploration for Studying Polarized Sections in Oil and Gas Geophysics. Dr. Sci. Thesis [in Russian]. Irkutsk State Technical University, Irkutsk.

- Legeydo, P.Yu., Mandelbaum, M.M., Rykhliniy, N.I., 1995. Differential-normalized method of electrical exploration in a direct search for hydrocarbon deposits. *Geofizika*, No. 4, 42–45.
- Legeydo, P.Yu., Mandelbaum, M.M., Rykhliniy, N.I., 1997. Informativeness of differential methods of electrical exploration in the study of polarizing media. *Geofizika*, No. 3, 49–56.
- Matveev, B.K., 1990. *Electrical Exploration* [in Russian]. Nedra, Moscow.
- Mogilatov, V.S., 2014. *Pulsed Electrical Exploration* [in Russian]. NGU, Novosibirsk.
- Moiseev, V.S., 2002. *Induced Polarization in the Search for Potentially Oil Bearing Areas* [in Russian]. Nauka, Novosibirsk.
- Nabighian M.N., 1979. Quasi-static transient response of a conducting half-space – An approximate representation. *Geophysics* 44, 1700–1705.
- Petrov, A.A., 2000. The possibilities of the TEM in a search for hydrocarbons in shelf zones. *Geofizika*, No. 5, 21–26.
- Sidorov, V.A., 1987. Electric polarizability of heterogeneous rocks. *Izv. Akad. Nauk SSSR. Fizika Zemli*, No. 10, 58–64.
- Strack K.-M., 1992. *Exploration with Deep Transient Electromagnetics*. Elsevier, Amsterdam.
- Vishnyakov, A.E., Lisitsyn, E.D., Yanevich, M.Yu., 1988. Influence of time parameters of induced polarization of hydrocarbon deposits on electromagnetic field transients, in: *Technique and Methodology of Geophysical Research of the World Ocean* [in Russian]. *Sevmorgeologiya*, Leningrad, pp. 124–132.
- Zhdanov, M.S., 2012. *Geophysical Electromagnetic Theory and Methods* [in Russian]. Nauchnyi Mir, Moscow.

Editorial responsibility: I.N. Yeltsov